Kennesaw State University
DigitalCommons@Kennesaw State University

Faculty Publications

2-20-1999

A Dynamical Study of the Non-Star-forming Translucent Molecular Cloud MBM 16: Evidence for Shear-driven Turbulence in the Interstellar Medium

Ted La Rosa
Kennesaw State University, tlarosa1@kennesaw.edu

Steven N. Shore
Indiana University - South Bend

Loris Magnani
University of Georgia

Follow this and additional works at: http://digitalcommons.kennesaw.edu/facpubs

 Part of the Stars, Interstellar Medium and the Galaxy Commons

Recommended Citation

LaRosa TN, Shore SN, Magnani L. 1999. A dynamical study of the non-star-forming translucent molecular cloud MBM 16: Evidence for smear-driven turbulence in the interstellar medium. Astrophys J 512(2):761-7.

This Article is brought to you for free and open access by DigitalCommons@Kennesaw State University. It has been accepted for inclusion in Faculty Publications by an authorized administrator of DigitalCommons@Kennesaw State University. For more information, please contact digitalcommons@kennesaw.edu.

THE ASTROPHYSICAL JOURNAL, 512:761–767, 1999 February 20
© 1999. The American Astronomical Society. All rights reserved. Printed in U.S.A.

A DYNAMICAL STUDY OF THE NON–STAR-FORMING TRANSLUCENT MOLECULAR CLOUD MBM 16: EVIDENCE FOR SHEAR-DRIVEN TURBULENCE IN THE INTERSTELLAR MEDIUM

T. N. LAROSA,[1] STEVEN N. SHORE,[2] AND LORIS MAGNANI[3]

Received 1998 May 28; accepted 1998 September 24

ABSTRACT

We present the results of a velocity correlation study of the high-latitude cloud MBM 16 using a fully sampled ^{12}CO map, supplemented by new ^{13}CO data. We find a correlation length of 0.4 pc. This is similar in size to the formaldehyde clumps described in our previous study. We associate this correlated motion with coherent structures within the turbulent flow. Such structures are generated by free shear flows. Their presence in this non–star-forming cloud indicates that kinetic energy is being supplied to the internal turbulence by an external shear flow. Such large-scale driving over long times is a possible solution to the dissipation problem for molecular cloud turbulence.

Subject headings: ISM: clouds — ISM: individual (MBM 16) — ISM: kinematics and dynamics — ISM: molecules — stars: formation — turbulence

1. INTRODUCTION

Superthermal line widths are commonly observed in molecular clouds, whether self-gravitating or not. Both internal and external driving mechanisms have been suggested as the source of these velocities (cf. Norman & Silk 1980; Fleck 1983; Henriksen & Turner 1984; Falgarone & Puget 1986; Scalo 1987; Mouschovias 1987; Myers & Goodman 1988; Falgarone & Phillips 1990; Elmegreen 1990; Passot et al. 1995). Virtually every suggested mechanism for producing the observed line widths requires mass motions and/or nonlinear wave motions, both of which are dissipative (Field 1978; Zweibel & Josafatsson 1983; Ghosh, Vinas, & Goldstein 1994). Recent simulations by Mac Low et al. (1998) and Padoan (1998) find that MHD turbulence decays on shorter timescales than previously thought. Thus, interstellar turbulence requires continuous injection of kinetic energy. The most obvious source in large clouds is internal star formation. There is, however, a type of molecular cloud, the high-latitude translucent variety (van Dishoeck et al. 1991), that shows the same superthermal velocity fields but does not display evidence of star-forming activity (e.g., Magnani et al. 1995). In the absence of internal driving mechanisms, such as star formation or gravity, the motion must be continually produced by an *external* agent.

It is for this reason that we have carried out a dynamical study of the translucent molecular cloud MBM 16 (Magnani, Blitz, & Mundy 1985, hereafter MBM). Our choice of this cloud is quite deliberate. In our earlier paper (Magnani, LaRosa, & Shore 1993, hereafter MLS93) we reported finding several large-scale formaldehyde clumps in MBM 16. These observations in H_2CO indicate that the clumps have a higher density than the rest of the cloud. We concluded that MBM 16 is not self-gravitating and that its internal structures are transient. Each clump has a distinct average centroid velocity that differs from the others by about 0.5 km s^{-1}. The difference is not due to a large-scale systematic motion. To quantify this, we have examined the standard statistical measures for the line profiles. The velocity centroid dispersion within each clump, $\sigma_c(H_2CO)$ in the notation of Kleiner & Dickman (1985 and references therein), was found to be quite low, <0.2 km s^{-1}, relative to the cloud as a whole determined from ^{12}CO data, 0.44 km s^{-1}, and relative to the clump-to-clump centroid velocity difference of 0.5 km s^{-1}. The CO data were, however, based on a severely undersampled map. In this study, we present the results of a more extensive ^{12}CO map of the cloud supplemented by new ^{13}CO observations of the densest formaldehyde clump that support and extend our earlier conclusions.

2. OBSERVATIONS

A complete map of MBM 16 was made in the ^{12}CO ($J = 1$–0) transition using the 1.2 m Harvard-Smithsonian Center for Astrophysics Millimeter Wave Telescope. The telescope front-end configuration is described by Dame (1995). The map is a $6^\circ \times 6^\circ$ grid in Galactic longitude and latitude ($\ell = 168^\circ$–174° and $b = -34^\circ$ to -40°) approximately centered on the cloud. The beamwidth of the telescope at 115 GHz is 8.′4, and the separation between the samples was 3.′6 for a total of 97×97 points or 9409 spectra. At the assumed cloud distance of 80 pc (Hobbs et al. 1988) 8.′4 corresponds to a linear resolution of 0.2 pc. The data were taken in frequency-switched mode at a velocity resolution of 0.65 km s^{-1}. The total bandwidth was 150 km s^{-1} centered at 0 km s^{-1} with respect to the LSR. Typical rms noise values for each spectrum were in the 0.133–0.281 K range.

A contour map of the integrated antenna temperature ($\int T_A^* \, dv$) is shown in Figure 1. The velocity map is shown in Figure 2. MBM 16 is clearly centered in the map and is completely enclosed by the mapping pattern. The general shape of the cloud is similar to the poorly sampled map by MBM, and the ragged structure is reminiscent of other high-latitude clouds. At the bottom left of the field in Figure 1 is a heretofore unidentified high-latitude cloud. Since the LSR velocity of the new cloud is significantly different from that of MBM 16, it is likely that the two clouds are at different distances. The molecular gas making up MBM 16 ranges in velocity from 4 to 10 km s^{-1}, while the new cloud

[1] Department of Biological and Physical Sciences, Kennesaw State University, 1000 Chastain Road, Kennesaw, GA 30144; ted@avatar.kennesaw.edu.

[2] Department of Physics and Astronomy, Indiana University South Bend, 1700 Mishawaka Avenue, South Bend, IN 46634-7111; sshore@paladin.iusb.edu.

[3] Department of Physics and Astronomy, University of Georgia, Athens, GA 30602; loris@zeus.physast.uga.edu.

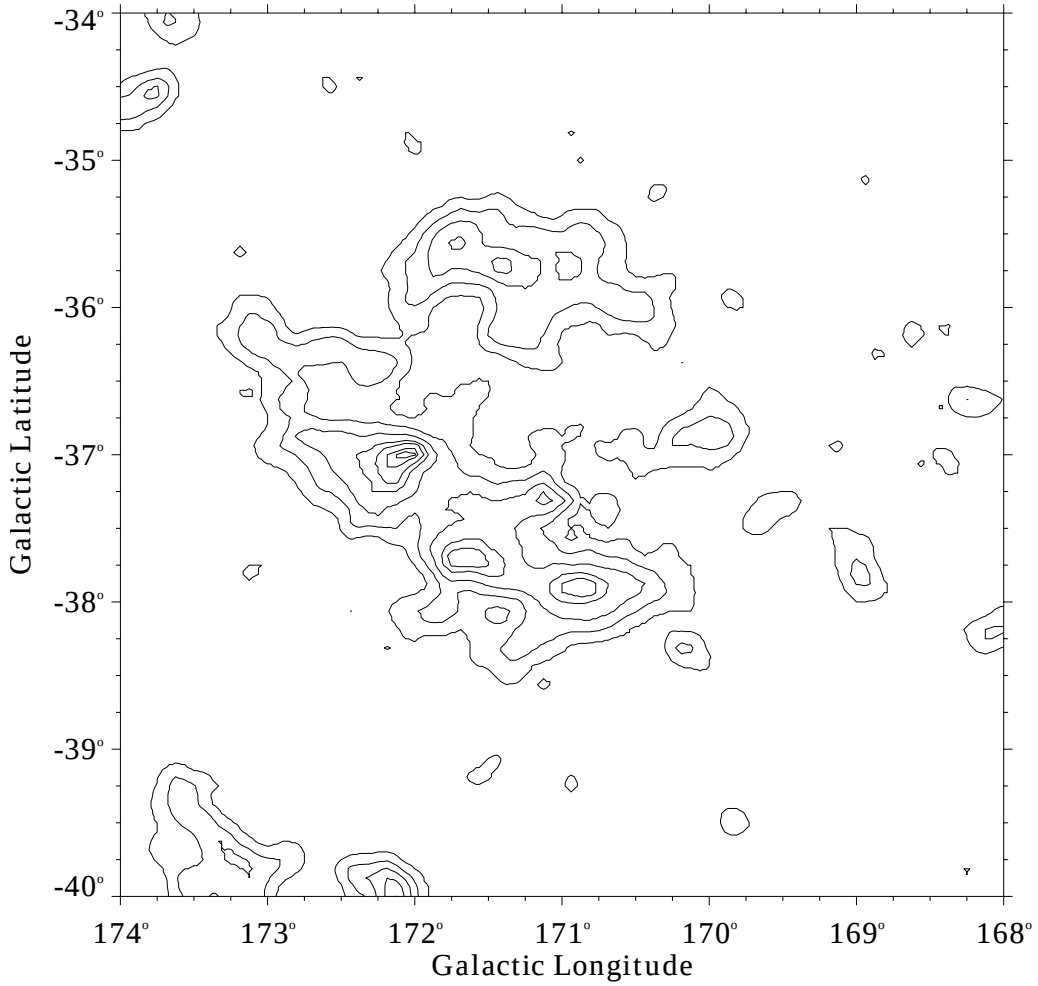

FIG. 1.—^{12}CO $J = 1$–0 contour map of a $6^\circ \times 6^\circ$ region centered on MBM 16. The velocity range of the map is -10 km s$^{-1} \leq v_{\rm LSR} \leq 15$ km s^{-1}. The contours are at [10, 30, 50, 70, 80, 90, and 95] percent of the maximum CO intensity of 7.23 K km s^{-1}. The objects to the extreme northeast and southeast of the map are probably not associated with MBM 16 (see text). The size of the 8.′4 beam, the effective map resolution, is shown in the upper right-hand corner.

LSR velocities lie between -20 and -5 km s^{-1}. Similarly, in the northeast corner of Figure 1 is a molecular feature that has LSR velocities in the 12–14 km s^{-1} range. CO channel maps of this region indicate that this feature is also likely to be a separate molecular cloud (Magnani et al. 1998, in preparation).

We have also mapped the largest formaldehyde clump and a portion of another in ^{13}CO at higher resolution than

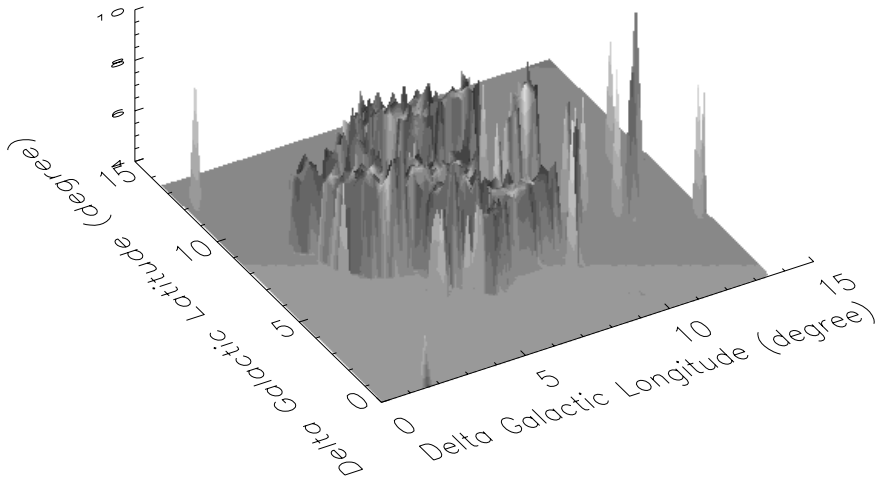

FIG. 2.—^{12}CO velocity map corresponding to the cloud shown in Fig. 1. This map corresponds to the velocity range 4–10 km s^{-1}. The orientation is the same as Fig. 1. One lag corresponds to 3.′6 for the fully sampled map.

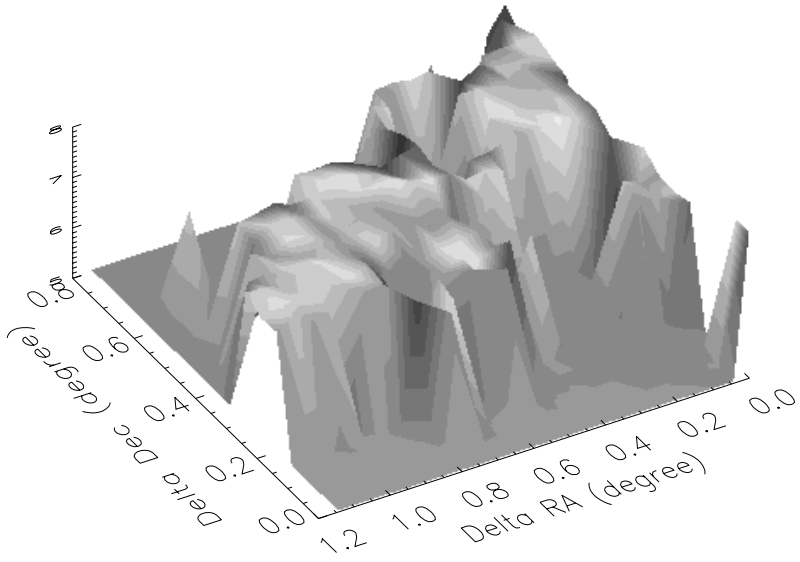

FIG. 3.—^{13}CO ($J = 1$–0) velocity map of a subregion in MBM 16. The (0, 0) location corresponds to (α, δ) = ($3^h21^m48^s$, 10°42′00″ in 1950 coordinates. The region covered by the map encompasses all of clump 3 and the eastern portion of clump 2 as defined in MLS93. The sampling is every 3′ with a 1′ beam, and the surface plot shows all velocities greater than 5 km s^{-1} (maximum is 8 km s^{-1}).

we reported in MLS93. These data were obtained during two observing sessions at the NRAO[4] 12 m telescope at Kitt Peak, Arizona, 1992 December 26–1993 January 1 and 1993 July 2–7. The 3 mm receiver with an SIS mixer operated with a total system plus sky temperature between 300 and 700 K. Dual polarizations were fed into a 100 kHz filter back end, providing a velocity resolution of 0.26 km s^{-1}. The data were obtained in frequency-switched mode with separation of ± 2 MHz. The polarizations were averaged together, and the resulting spectrum was folded resulting in typical rms noise temperatures from 10 to 30 mK after Hann smoothing. We used a uniformly spaced 20 × 27 grid with 3′ separation between beam centers (the beam size is $\sim 1'$ at 113 GHz). The map concentrated primarily on clump 3 in the H_2CO study described by MLS93, although a portion of clump 2 was included in the western section of the map. The integrated ^{13}CO ($J = 1$–0) intensity map of the region is shown in Figure 3. Line emission was detected in about 200 of the 540 map positions.

3. STATISTICAL AND CORRELATION ANALYSES

For fully developed turbulence over a large enough region the dispersion in the centroid velocities should be about the same as the individual line widths. The ^{13}CO data agree with the H_2CO results in showing a much smaller centroid dispersion within the clumps. Following Kleiner & Dickman (1985), for the entire sampled cloud the parent velocity dispersion of the mapped region, σ_p, i.e., the average dispersion of the individual spectra, σ_i, is 0.25 km s^{-1} and the dispersion in the intensity-weighted velocity centroids determined from Gaussian profile fitting, σ_c, is 0.31 km s^{-1}. For the leftmost clump located at $\Delta RA \geq 50.25$ in Figure 3, $\sigma_i = 0.21$ and $\sigma_c = 0.10$ km s^{-1}. The implication is that the clumps are coherent in velocity. The ^{13}CO map is, however, too small to be useful for a correlation study. Our new ^{12}CO map is fully sampled and sufficiently large to permit such an analysis.

The velocity correlation function is the simplest description of the dynamical properties of a flow. By definition, the spatial velocity correlation function for a homogeneous turbulent flow is

$$c_{ii}(\tau) = \langle [v_i(r) - \langle v_i(r) \rangle][v_i(r + \tau) - \langle v_i(r) \rangle] \rangle , \quad (1)$$

where the angle brackets denote the spatial averages. The lag, τ, is a scalar quantity. We are, of course, limited to measuring only the radial velocities so we can construct only the longitudinal velocity autocorrelation along the line of sight, $c_{zz}(\tau)$. We normalize the autocorrelation function by its value at zero lag, $C(\tau) = c_{zz}(\tau)/c_{zz}(0)$. In standard terminology, this is known as the biased autocorrelation function (see Miesch & Bally 1994, hereafter MB94).

Before performing the autocorrelation analysis, we trimmed the data to remove points in the map with velocities that are clearly in excess of the bulk of the cloud. In this case, we retained all points with a signal-to-noise ratio of 4.5 σ or higher with 4.0 km s^{-1} $\leq v_{rad} \leq$ 10.0 km s^{-1}, the range of velocities found within MBM 16.

As discussed by Scalo (1984) and further elaborated by MB94, any correlation analysis requires some filtering of the data set to remove the large-scale trends. Therefore, we have applied two different methods to the MBM 16 data. In the first procedure we subtracted the mean velocity, 7.24 km s^{-1}, from the trimmed map to form the fluctuation map. In the second procedure we subtracted a smoothed map from the data that were obtained from the trimmed map by taking a running mean filter of preset size that included only detected points. This is the procedure used by Miesch & Bally. We then carried out the autocorrelation analysis of these filtered ^{12}CO data using two independent methods. The first, which is identical to the one described by MB94, used the two-dimensional fast Fourier transform in interactive data language. For comparison, in the second we used the scalar algebraic correlation function.

The results are plotted in Figures 4 and 5. Figures 4*a*–4*c* shows the two-dimensional correlation results for (*a*) the

[4] The National Radio Astronomy Observatory is operated by Associated Universities, Inc., in a cooperative agreement with the National Science Foundation.

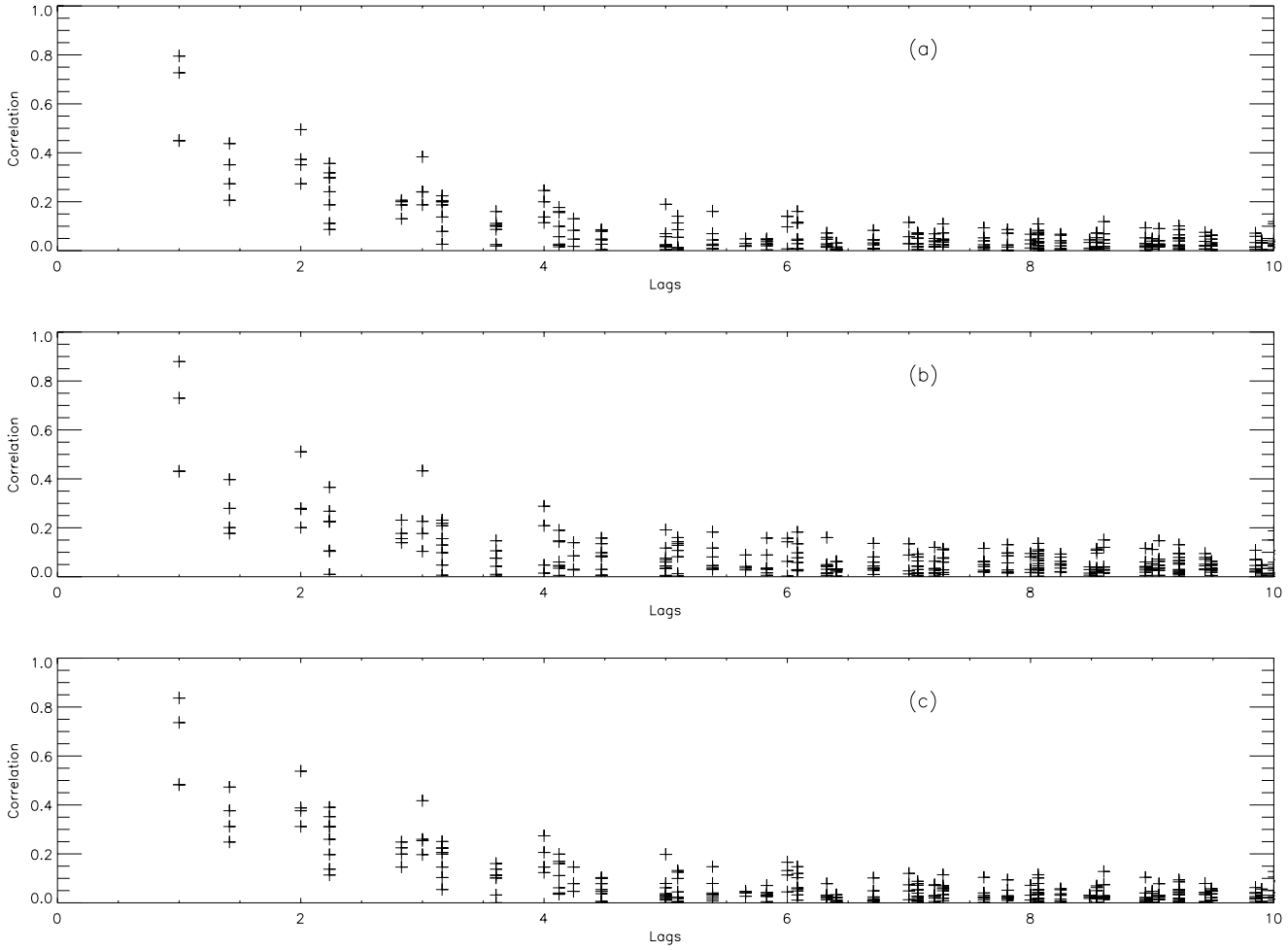

FIG. 4.—Two-dimensional velocity correlation function for different normalizations (see text) obtained by (*a*) subtracting a constant mean for the cloud of 7.24 km s^{-1}; (*b*) subtracting a smoothed map with a 15 point running mean; and (*c*) subtracting a 30 point running mean.

mean-subtracted, (*b*) the 15 point smoothed, and (*c*) the 30 point smoothed maps. In view of the agreement between the different procedures, and the lack of systematic trends in the velocity, we use the method of Figure 4*a* for Figure 5 and the subsequent analysis. In Figure 5, we show the comparison between the scalar (one-dimensional) and two-dimensional correlation functions for the mean-subtracted map. The two methods agree. There is a detectable correlation up to five lags or 18.′0, which corresponds to a physical length of 0.42 pc.[5] To further understand what the correlation function is measuring, and in particular how to define the correlation length, we performed a series of simulations the results for which are shown in Figure 6. To generate a test random map with the same spatial distribution as the real data, we took the trimmed map, normalized it to unity for all detections, and then multiplied each detected location by a Gaussian random number with a unit dispersion. The correlation function for this completely random map is shown in Figure 6*a*. Notice that although the velocity is spatially confined to the regions where CO was detected, there is no hint of any spatial structure in the figure. We then simulated the presence of a coherent structure within this map by setting all velocities in a 10×10 region equal to a constant and, in a series of trials, varied the constant. This creates a coherently moving clump of known size and kinetic energy. The velocity was increased from 0 to 2 km s^{-1} to produce a set of maps that were then run through the same analysis as the real data. What they show is that there are clear limits to the information that can be derived from a correlation analysis but that the detection of a correlated flow is possible.

For instance, in Figures 6*b*–6*d*, the amplitude of the velocity was increased from 0.5 to 2.0 km s^{-1} where the random map has velocities in the range -6.3 to 4.4 km s^{-1}. Again, we note that the velocity dispersion was 1 km s^{-1}. With an amplitude of 0.5 km s^{-1}, the clump had about 3% of the total power in the map and the structure was clearly undetectable (Fig. 6*b*). For 1 km s^{-1}, or about 13% of the total power, the structure is obvious (Fig. 6*c*) and becomes more so with increasing energy. An additional result of the simulations is that the size of the coherent region is not the e^{-1} point but is where the correlation function has its first zero (e.g., Townsend 1976). More important is the result that the lack of detection of a coherent region by the corre-

[5] This is about 2.5 beamwidths. We used the same random maps described below to test the effects of beam size on our derived correlation functions. For example, for a Gaussian beamwidth (FWHM) of four lags convolved with the random map, the correlation function has its first zero at two lags. The same map convolved with our beam size yielded no correlation above one lag. Therefore, tests show that the correlation we are reporting here does not arise as an artifact of the sampling.

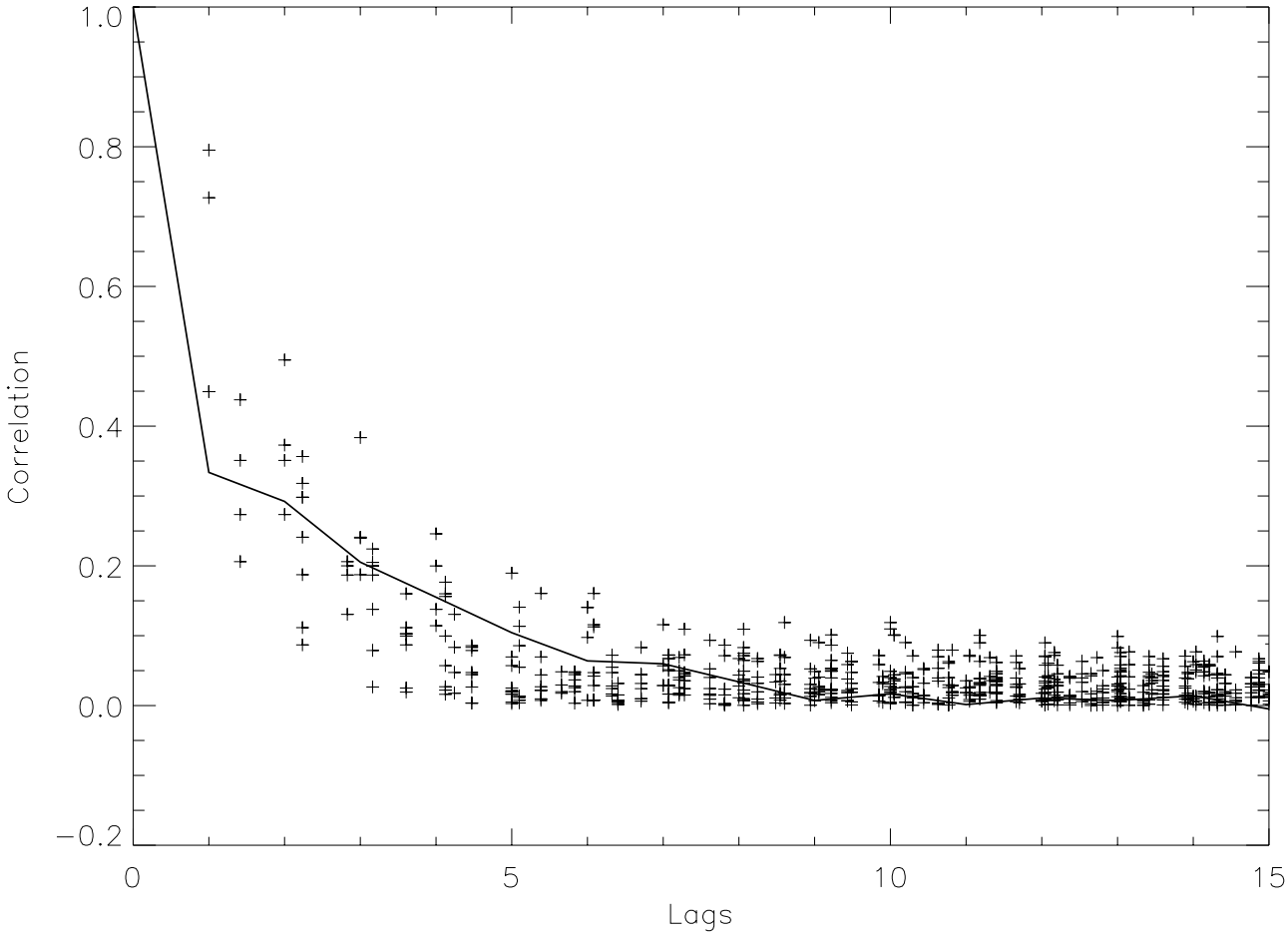

FIG. 5.—Comparison of the one- and two-dimensional velocity correlation functions for the mean-subtracted data. Note that the scalar correlation function, the solid line in the figure, is *not* a fit to the points.

lation method merely places an upper limit on the size and power of such regions but does not rule out their presence.

4. DISCUSSION

On the basis of a purely statistical analysis of the line profiles for a number of molecular species, ^{12}CO, ^{13}CO, and H_2CO, it is clear that MBM 16 contains a number of regions with exceptionally low dispersions in the line centroid velocity. We emphasize that these are not simply "quiet spots" in the flow. The individual profiles throughout these regions have the same widths as the rest of the cloud, which is much larger than the dispersion in the centroids. The implication of this observation is that the size–line width relation (Larson 1981) breaks down for this cloud. This is shown in detail in Figure 7. There is no systematic trend to the data, and those regions identified by MLS93 from the formaldehyde observations clearly stand out in the ^{12}CO data as anomalously underdispersed for their size.

The results of our correlation analysis support and strengthen these statistical conclusions. We find a correlation length of roughly 18′, corresponding to a physical scale of about 0.4 pc. Our simulations suggest that these regions must together contain at least 10% of the kinetic energy of the cloud. We argue that these regions are the interstellar analogs of the *coherent structures* that usually accompany turbulence generated in free and bounded shear flows. These have been the subject of increasing attention in the past few years as their importance in turbulence has been more clearly recognized in terrestrial flows (e.g., Lumley 1989; George & Arendt 1989; Robinson 1991; McComb 1991; Shore 1992; Gutmark, Schadow, & Yu 1995; Holmes, Lumley, & Berkooz 1996).

In the most general case where the flow can be driven both internally and externally, it is likely that no single source scale would be detected using correlation methods because none exists. Instead, the variety of processes acts on so many different scales that no one process produces a clean dynamical signature. As far we know, there have been no previous dynamical studies of any *isolated* non–star-forming cloud.[6] It is therefore not surprising that no unambiguous velocity correlation length is generally found (e.g., MB94). Scalo (1984) suggested that a length scale of order 0.3 pc in the ρ Oph cloud might be due to turbulence, although it was possible that large-scale structure could produce a similar signature. It is precisely the simplicity of the velocity field in MBM 16 that makes such a detection more likely if it exists. This cloud is nearby so we can obtain fully sampled maps of comparatively small scale structures. More important, the lack of internal sources for turbulence

[6] Although Heiles 2 and other non–star-forming clouds have been observed, these are all associated with or embedded within larger star-forming cloud complexes. MBM 16 is completely isolated.

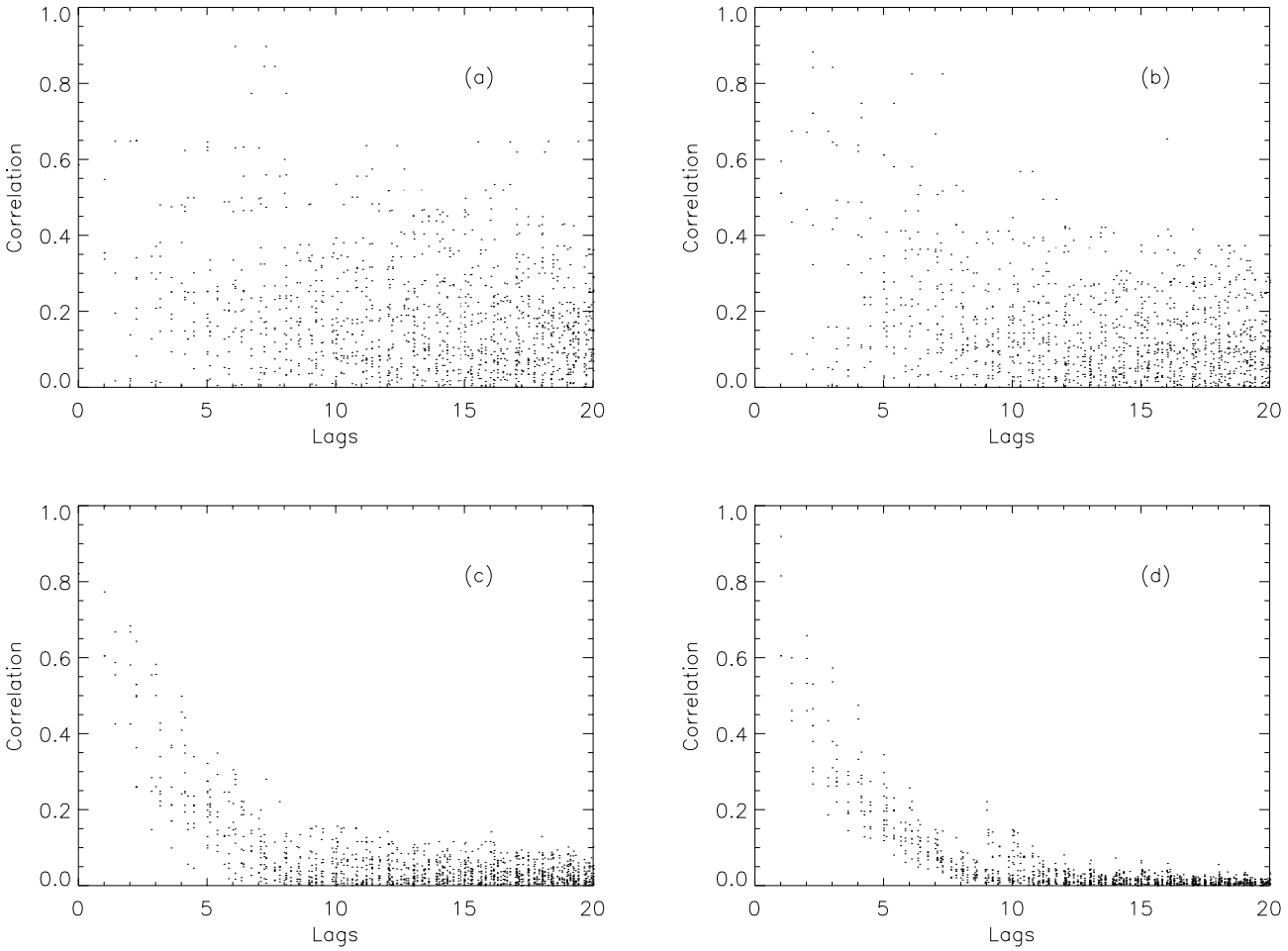

FIG. 6.—Results of simulations of a coherent structure in a normally distributed velocity fluctuation map. The figure shows the two-dimensional velocity correlation function for simulations described in the text with (*a*) $\Delta v = 0$ km s^{-1}; (*b*) 0.5 km s^{-1}; (*c*) 1.0 km s^{-1}; (*d*) 2 km s^{-1}.

in MBM 16 means that any external driver will leave a recognizable signature in the velocity field of the cloud.

If we are correct in assigning the source of the coherent structures to an external shear flow, then there are important consequences for the interpretation of the line profiles in this and other clouds. First, such phenomena should be ubiquitous in the interstellar medium. For instance, any H I cloud should show similar structures. Boundary layer effects have already been invoked in chemical studies of molecular clouds (e.g., Charnley et al. 1990). In particular, we suggest that a correlation analysis of a high-velocity H I cloud might reveal coherent structures generated by boundary shear with the interstellar medium.[7] Second, such driven turbulence will produce MHD waves so long as the fluid and magnetic field are coupled. This is true throughout the interstellar medium. Third, the fact that large-scale external driving can feed the observed internal motions points to a long-lived source. Even though both MHD waves and turbulence are intrinsically dissipative, the longevity of the driver can overcome the dissipation and maintain the stability of the clouds for very long times. Thus, the detection of turbulence does not imply any particular youth for the clouds.

[7] Recent analytic and numerical work by Vietri, Ferrara, & Miniati (1997) suggests that non–self-gravitating clouds are not disrupted by the Kelvin-Helmholtz instability.

5. SUMMARY

Our purpose in this paper has been to characterize the velocity field within a non–star-forming molecular cloud. We were guided by earlier H_2CO observations at 6′ resolution (0.14 pc) that showed dynamical ordering on a length scale of about 0.5 pc. Using higher resolution and a far more complete ^{12}CO map, we find evidence for a velocity correlation on a scale of 0.4 pc. We attribute this to the formation of coherent structures in an externally driven turbulent shear flow. This could easily be the source for both MHD and fluid turbulence on a small scale within this and other molecular clouds[8] and could supply kinetic energy to the clouds on potentially long timescales.

We thank Paul Hart, Tom Fokkers, and Dale Emerson, without whose expert help the observations would not have happened. We also thank John Scalo for extensive and selfless advice and correspondence and Tom Harquist, the referee, for his advice. We also thank Ellen Zweibel, Alyssa Goodman, Enrique Vázquez-Semadeni, Bruce Elmegreen, Jose Franco, and Michael Pérault for discussions. We

[8] This explanation may specifically apply to giant molecular clouds. For instance, Williams, Blitz, & Stark (1995) have observed numerous clumped structures in turbulent clouds that do not contain embedded stars yet otherwise display the same turbulence properties as we have discussed here. We thank the referee, T. Harquist, for suggesting this addition.

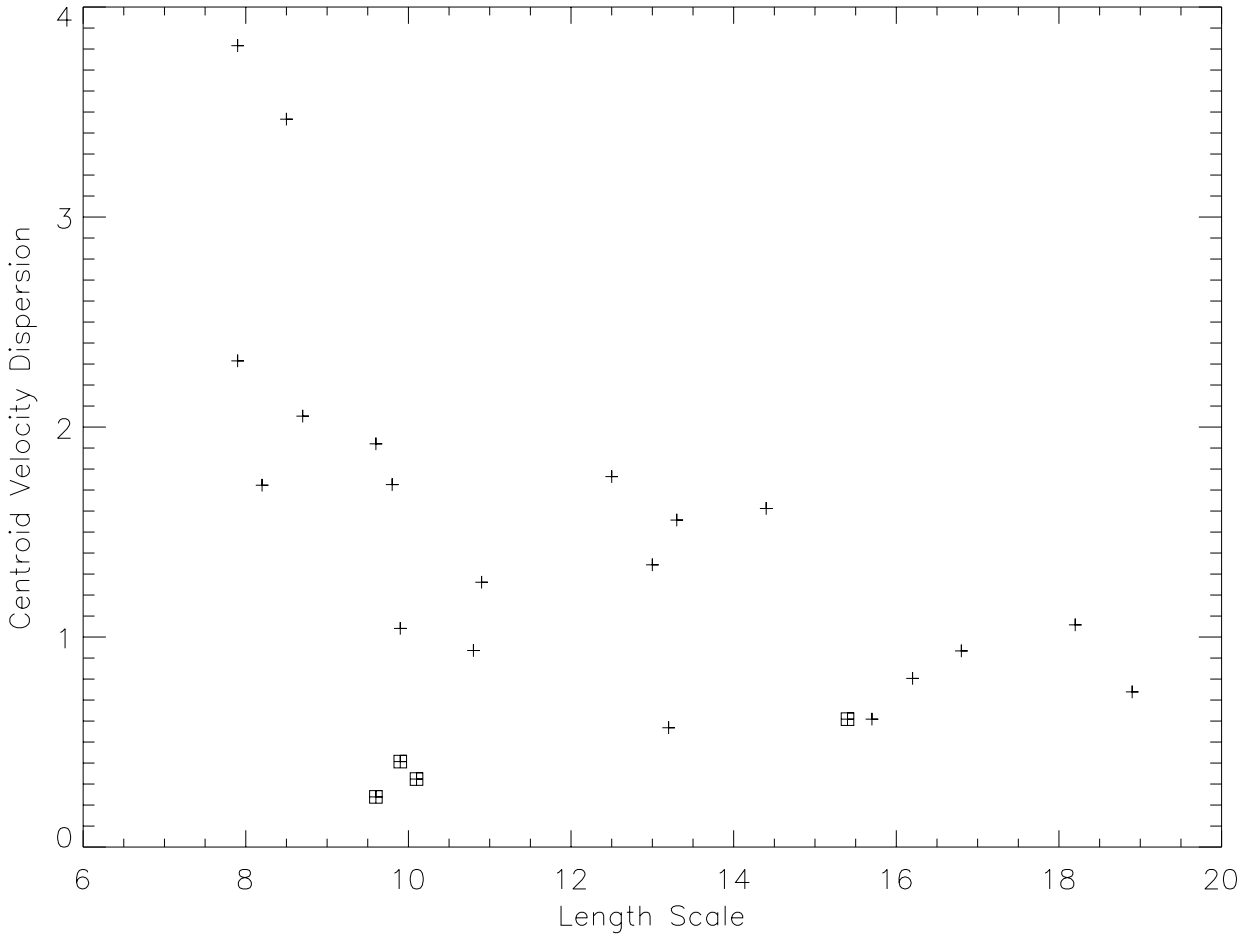

FIG. 7.—Size–line width results for the ^{12}CO data for MBM 16. The squares represent the H_2CO clumps, while the crosses are for regions throughout the cloud. The length scale is the square root of the number of detected points within the sampled region. The centroid velocity dispersion was determined from the intensity-weighted centroids of the individual line profiles. Notice the distinct separation of the clumps from the bulk of the data and the absence of any obvious overall trend.

thank Dap Hartmann for help with the figures of the ^{12}CO observations. T. N. L. is supported by a NASA JOVE grant to Kennesaw State University. S. N. S. is partially funded by NASA.

REFERENCES

Charnley, S. B., Dyson, J. E., Hartquist, T. W., & Williams, D. A. 1990, MNRAS, 243, 405
Dame, T. M. 1995, Calibration of the 1.2 Meter Telescopes: Internal Report No. 4, Harvard-Smithsonian CfA
Elmegreen, B. G. 1990, ApJ, 361, L77
Falgarone, E., & Phillips, T. G. 1990, ApJ, 359, 344
Falgarone, E., & Puget, J.-L. 1986, A&A, 162, 235
Field, G. 1978, in Protostars and Planets, ed. T. Gehrels & M. S. Shapley (Tucson: Univ. Arizona Press), 243
Fleck, R. C., Jr. 1983, ApJ, 272, L45
George, W. K., & Arndt, R. (eds). 1989, Advances in Turbulence (New York: Hemisphere)
Ghosh, S., Vinas, A. F., & Goldstein, M. L. 1994, JGR, 99, 19289
Gutmark, E. J., Schadow, K. C., & Yu, K. H. 1995, Ann. Rev. Fluid Mech., 27, 375
Henriksen, R. J., & Turner, B. E. 1984, ApJ, 287, 200
Hobbs, L. M., et al. 1988, ApJ, 327, 356
Holmes, P., Lumley, J. L., & Berkooz, G. 1996, Turbulence, Coherent Structures, Dynamical Systems and Symmetry (Cambridge: Cambridge Univ. Press)
Kleiner, S. C., & Dickman, R. L. 1985, ApJ, 295, 466
Larson, R. B. 1981, MNRAS, 194, 809
Lumley, J. L. 1989, Advances in Turbulence, ed. W. K. George & R. Arndt (New York: Hemisphere), 6
Mac Low, M.-M., Klessen, R. S., Burkhert, A., & Smith, M. D. 1998, Phys. Rev. Lett., 80, 2754
Magnani, L., Blitz, L., & Mundy, L. 1985, ApJ, 402, 295 (MBM)
Magnani, L., Caillault, J.-P., Buchalter, A., & Beichman, C. A. 1995, ApJS, 95, 159
Magnani, L., LaRosa, T. N., & Shore, S. N. 1993, ApJ, 402, 226 (MLS93)
McComb, W. D. 1991, The Physics of Fluid Turbulence (New York: Oxford Univ. Press)
Miesch, M. S. & Bally, J. 1994, ApJ, 429, 645 (MB94)
Mouschovias, T. Ch. 1987, Physical Processes in Interstellar Clouds, ed. G. Morfill & M. Scholer (Dordrecht: Reidel), 453
Myers, P. C., & Goodman, A. A. 1988, ApJ, 329, 392
Norman, C., & Silk, J. 1980, ApJ, 238, 158
Padoan, P. 1998, in Interstellar Turbulence, Proc. Second Gulliermo Conf., ed. J. Franco & A. Carraminana (Cambridge: Cambridge Univ. Press), in press
Passot, T., Vazquez-Semadeni, E., & Pouquet, A. 1995, ApJ, 455, 536
Robinson, K. 1991, Ann. Rev. Fluid Mech., 23, 601
Scalo, J. M. 1984, ApJ, 277, 566
———. 1987, in Interstellar Processes, ed. D. J. Hollenbach & H. A. Thronson, Jr. (Dordrecht: Reidel), 347
Shore, S. N. 1992, An Introduction to Astrophysical Hydrodynamics (San Diego: Academic)
Townsend, A. A. 1976, The Structure of Turbulent Shear Flow (Cambridge: Cambridge Univ. Press)
van Dishoeck, E. F., Black, J. H., Phillips, T. G., & Gredel, R. 1991, ApJ, 366, 141
Vietri, M., Ferrara, A., & Miniati, F. 1997, ApJ, 483, 262
Williams, J. P., Blitz, L., & Stark, A. A. 1995, ApJ 451, 252
Zweibel, E. G., & Josafatsson, K. 1983, ApJ, 270, 511